Robust Adaptive Beamforming

Edited by

Jian Li and Petre Stoica

A JOHN WILEY & SONS, INC., PUBLICATION

Robust Adaptive Beamforming

Robust Adaptive Beamforming

Edited by

Jian Li and Petre Stoica

A JOHN WILEY & SONS, INC., PUBLICATION

Published by John Wiley & Sons, Inc., Hoboken, New Jersey.
Published simultaneously in Canada.

Library of Congress Cataloging-in-Publication Data:

Robust adaptive beamforming/edited by Jian Li and Petre Stoica.
p. cm.
Includes bibliographical references and index.
ISBN-13 978-0-471-67850-2 (cloth)
ISBN-10 0-471-67850-3 (cloth)
1. Adaptive antennas. 2. Antenna radiation patterns. I. Li, Jian. II. Stoica, Petre.

TK7871.67.A33R63 2005
621.382′4--dc22 2004065908

Printed in the United States of America

10 9 8 7 6 5 4 3 2 1

CONTENTS

Contributors ix

Preface xi

1 Robust Minimum Variance Beamforming 1
Robert G. Lorenz and Stephen P. Boyd

1.1 Introduction 1
1.2 A Practical Example 8
1.3 Robust Weight Selection 12
1.4 A Numerical Example 23
1.5 Ellipsoidal Modeling 28
1.6 Uncertainty Ellipsoid Calculus 31
1.7 Beamforming Example with Multiplicative Uncertainties 41
1.8 Summary 44
Appendix: Notation and Glossary 44
References 45

2 Robust Adaptive Beamforming Based on Worst-Case Performance Optimization 49
Alex B. Gershman, Zhi-Quan Luo, and Shahram Shahbazpanahi

2.1 Introduction 49
2.2 Background and Traditional Approaches 51
2.3 Robust Minimum Variance Beamforming Based on Worst-Case Performance Optimization 60
2.4 Numerical Examples 74
2.5 Conclusions 80
Appendix 2.A: Proof of Lemma 1 81
Appendix 2.B: Proof of Lemma 2 81
Appendix 2.C: Proof of Lemma 3 82
Appendix 2.D: Proof of Lemma 4 84
Appendix 2.E: Proof of Lemma 5 85
References 85

3 Robust Capon Beamforming **91**
Jian Li, Petre Stoica, and Zhisong Wang

3.1 Introduction 91
3.2 Problem Formulation 93
3.3 Standard Capon Beamforming 95
3.4 Robust Capon Beamforming with Single Constraint 96
3.5 Capon Beamforming with Norm Constraint 112
3.6 Robust Capon Beamforming with Double Constraints 116
3.7 Robust Capon Beamforming with Constant Beamwidth and Constant Powerwidth 133
3.8 Rank-Deficient Robust Capon Filter-Bank Spectral Estimator 148
3.9 Adaptive Imaging for Forward-Looking Ground Penetrating Radar 166
3.10 Summary 185
Acknowledgments 185
Appendix 3.A: Relationship between RCB and the Approach in [14] 185
Appendix 3.B: Calculating the Steering Vector 188
Appendix 3.C: Relationship between RCB and the Approach in [15] 189
Appendix 3.D: Analysis of Equation (3.72) 190
Appendix 3.E: Rank-Deficient Capon Beamformer 191
Appendix 3.F: Conjugate Symmetry of the Forward-Backward FIR 193
Appendix 3.G: Formulations of NCCF and HDI 194
Appendix 3.H: Notations and Abbreviations 195
References 196

4 Diagonal Loading for Finite Sample Size Beamforming: An Asymptotic Approach **201**
Xavier Mestre and Miguel A. Lagunas

4.1 Introduction and Historical Review 202
4.2 Asymptotic Output SINR with Diagonal Loading 213
4.3 Estimating the Asymptotically Optimum Loading Factor 225
4.4 Characterization of the Asymptotically Optimum Loading Factor 236
4.5 Summary and Conclusions 243
Acknowledgments 243
Appendix 4.A: Proof of Proposition 1 243
Appendix 4.B: Proof of Lemma 1 246
Appendix 4.C: Derivation of the Consistent Estimator 247
Appendix 4.D: Proof of Proposition 2 249
References 254

5 Mean-Squared Error Beamforming for Signal Estimation: A Competitive Approach **259**
Yonina C. Eldar and Arye Nehorai

5.1 Introduction 259
5.2 Background and Problem Formulation 261
5.3 Minimax MSE Beamforming for Known Steering Vector 271
5.4 Random Steering Vector 281
5.5 Practical Considerations 284
5.6 Numerical Examples 285
5.7 Summary 294
Acknowledgments 295
References 296

6 Constant Modulus Beamforming **299**
Alle-Jan van der Veen and Amir Leshem

6.1 Introduction 299
6.2 The Constant Modulus Algorithm 303
6.3 Prewhitening and Rank Reduction 307
6.4 Multiuser CMA Techniques 312
6.5 The Analytical CMA 315
6.6 Adaptive Prewhitening 325
6.7 Adaptive ACMA 328
6.8 DOA Assisted Beamforming of Constant Modulus Signals 338
6.9 Concluding Remarks 347
Acknowledgment 347
References 347

7 Robust Wideband Beamforming **353**
Elio D. Di Claudio and Raffaele Parisi

7.1 Introduction 353
7.2 Notation 357
7.3 Wideband Array Signal Model 358
7.4 Wideband Beamforming 363
7.5 Robustness 369
7.6 Steered Adaptive Beamforming 381
7.7 Maximum Likelihood STBF 389
7.8 ML-STBF Optimization 393
7.9 Special Topics 399
7.10 Experiments 401
7.11 Summary 410
Acknowledgments 411
References 412

Index **417**

CONTRIBUTORS

STEPHEN P. BOYD, Information Systems Laboratory, Stanford University, Stanford, CA 94305

ELIO D. DI CLAUDIO, INFOCOM Department, University of Roma "La Sapienza," Via Eudossiana 18, I-00184 Roma, Italy

YONINA C. ELDAR, Department of Electrical Engineering, Technion—Israel Institute of Technology, Haifa 32000, Israel

ALEX B. GERSHMAN, Darmstadt University of Technology, Institute of Telecommunications, Merckstrasse 25, 64283 Darmstadt, Germany

MIGUEL A. LAGUNAS, Centre Tecnològic de Telecomunicacions de Catalunya, NEXUS 1 Building, Gran Capita 2–4, 08034 Barcelona, Spain

AMIR LESHEM, School of Engineering, Bar-Ilan University, 52900 Ramat-Gan, Israel

JIAN LI, Department of Electrical and Computer Engineering, Engineering Bldg., Center Drive, University of Florida, Gainesville, FL 32611

ROBERT G. LORENZ, Beceem Communications, Santa Clara, CA 95054

ZHI-QUAN LUO, Department of Electrical and Computer Engineering, University of Minnesota, Minneapolis, MN 55455

XAVIER MESTRE, Centre Tecnològic de Telecomunicacions de Catalunya, NEXUS 1 Building, Gran Capita 2–4, 08034 Barcelona, Spain

ARYE NEHORAI, Department of Electrical Engineering and Computer Science, University of Illinois at Chicago, Chicago, IL 60607

RAFFAELE PARISI, INFOCOM Department, University of Roma "La Sapienza," Via Eudossiana 18, I-00184 Roma, Italy

SHAHRAM SHAHBAZPANAHI, McMaster University, Hamilton, Ontario L8S 4L8, Canada

PETRE STOICA, Division of Systems and Control, Department of Information Technology, Uppsala University, SE-75105 Uppsala, Sweden

ALLE-JAN VAN DER VEEN, Department of Electrical Engineering, Delft University of Technology, 2628 Delft, The Netherlands

ZHISONG WANG, Department of Electrical and Computer Engineering, Engineering Bldg., Center Drive, University of Florida, Gainesville, FL 32611

PREFACE

Beamforming is a ubitiquitous task in array signal processing with applications, among others, in radar, sonar, acoustics, astronomy, seismology, communications, and medical-imaging. The standard data-independent beamformers include the delay-and-sum approach as well as methods based on various weight vectors for sidelobe control. The data-dependent or adaptive beamformers select the weight vector as a function of the data to optimize the performance subject to various constraints. The adaptive beamformers can have better resolution and much better interference rejection capability than the data-independent beamformers. However, the former are much more sensitive to errors, such as the array steering vector errors caused by imprecise sensor calibrations, than the latter. As a result, much effort has been devoted over the past three decades to devise robust adaptive beamformers.

The primary goal of this edited book is to present the latest research developments on robust adaptive beamforming. Most of the early methods of making the adaptive beamformers more robust to array steering vector errors are rather ad hoc in that the choice of their parameters is not directly related to the uncertainty of the steering vector. Only recently have some methods with a clear theoretical background been proposed, which, unlike the early methods, make explicit use of an uncertainty set of the array steering vector. The application areas of robust adaptive beamforming are also continuously expanding. Examples of new areas include smart antennas in wireless communications, hand-held ultrasound imaging systems, and directional hearing aids. The publication of this book will hopefully provide timely information to the researchers in all the aforementioned areas.

The book is organized as follows. The first three chapters (Chapter 1 by Robert G. Lorenz and Stephen P. Boyd; Chapter 2 by Alex B. Gershman, Zhi-Quan Luo, and Shahram Shahbazpanahi; and Chapter 3 by Jian Li, Petre Stoica, and Zhisong Wang) discuss how to address directly the array steering vector uncertainty within a clear theoretical framework. Specifically, the robust adaptive beamformers in these chapters couple the standard Capon beamformers with a spherical or ellipsoidal uncertainty set of the array steering vector. The fourth chapter (by Xavier Mestre and Miguel A. Lagunas) concentrates on alleviating the finite sample size effect. Two-dimensional asymptotics are considered based on the assumptions that both the number of sensors and the number of observations are large and that they

have the same order of magnitude. The fifth chapter (by Yonina C. Eldar and Arye Nehorai) considers the signal waveform estimation. The mean-squared error rather than the signal-to-interference-plus-noise ratio is used as a performance measure. Two cases are treated, including the case of known steering vectors and the case of random steering vectors with known second-order statistics. The sixth chapter (by Alle-Jan van der Veen and Amir Leshem) focuses on constant modulus algorithms. Two constant modulus algorithms are put into a common framework with further discussions on their iterative and adaptive implementations and their direction finding applications. Finally, the seventh chapter (by Elio D. Di Claudio and Raffaele Parisi) is devoted to robust wideband beamforming. Based on a constrained stochastic maximum likelihood error functional, a steered adaptive beamformer is presented to adapt the weight vector within a generalized sidelobe canceller formulation.

We are grateful to the authors who have contributed to the chapters of this book for their excellent work. We would also like to acknowledge the contributions of several other people and organizations to the completion of this book. Most of our work in the area of robust adaptive beamforming is an outgrowth of our research programs in array signal processing. We would like to thank those who have supported our research in this area: the National Science Foundation, the Swedish Science Council (VR), and the Swedish Foundation for International Cooperation in Research and Higher Education (STINT). We also wish to thank George Telecki (Associate Publisher) and Rachel Witmer (Editorial Assistant) at Wiley for their effort on the publication of this book.

JIAN LI AND PETRE STOICA

1

ROBUST MINIMUM VARIANCE BEAMFORMING

Robert G. Lorenz
Beceem Communications, Santa Clara, CA 95054

Stephen P. Boyd
Information Systems Laboratory, Stanford University, Stanford, CA 94305

1.1 INTRODUCTION

Consider the n dimensional sensor array depicted in Figure 1.1. Let $a(\theta) \in \mathbf{C}^n$ denote the response of the array to a plane wave of unit amplitude arriving from direction θ; we shall refer to $a(\cdot)$ as the *array manifold*. We assume that a narrow-band source $s(t)$ is impinging upon the array from angle θ and that the source is in the far-field of the array. The vector array output $y(t) \in \mathbf{C}^n$ is then

$$y(t) = a(\theta)s(t) + v(t), \tag{1.1}$$

where $a(\theta)$ includes effects such as coupling between elements and subsequent amplification; $v(t)$ is a vector of additive noises representing the effect of undesired signals, such as thermal noise or interference. We denote the sampled array output by $y(k)$. Similarly, the combined beamformer output is given by

$$y_c(k) = w^* y(k) = w^* a(\theta)s(k) + w^* v(k)$$

where $w \in \mathbf{C}^n$ is a vector of weights, that is, design variables, and $(\cdot)^*$ denotes the conjugate transpose.

Robust Adaptive Beamforming, Edited by Jian Li and Petre Stoica

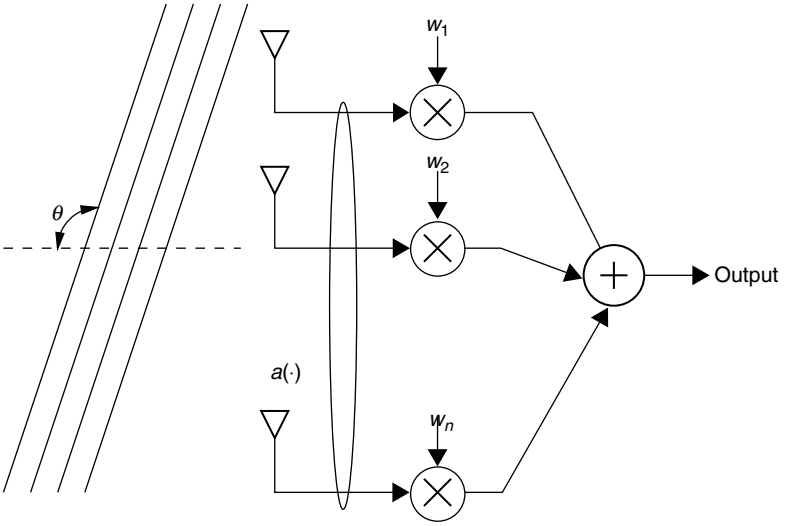

Figure 1.1 Beamformer block diagram.

The goal is to make $w^*a(\theta) \approx 1$ and $w^*v(t)$ small, in which case, $y_c(t)$ recovers $s(t)$, that is, $y_c(t) \approx s(t)$. The gain of the weighted array response in direction θ is $|w^*a(\theta)|$; the expected effect of the noise and interferences at the combined output is given by $w^*R_v w$, where $R_v = \mathbf{E}\, vv^*$ and $\mathbf{E}$ denotes the expected value. If we presume $a(\theta)$ and R_v are known, we may choose w as the optimal solution of

$$\begin{array}{ll} \text{minimize} & w^*R_v w \\ \text{subject to} & w^*a(\theta_d) = 1. \end{array} \tag{1.2}$$

Minimum variance beamforming is a variation on (1.2) in which we replace R_v with an estimate of the received signal covariance derived from recently received samples of the array output, for example,

$$R_y = \frac{1}{N} \sum_{i=k-N+1}^{k} y(i)y(i)^* \in \mathbf{C}^{n\times n}. \tag{1.3}$$

The minimum variance beamformer (MVB) is chosen as the optimal solution of

$$\begin{array}{ll} \text{minimize} & w^*R_y w \\ \text{subject to} & w^*a(\theta) = 1. \end{array} \tag{1.4}$$

This is commonly referred to as Capon's method [1]. Equation (1.4) has an analytical solution given by

$$w_{\mathrm{mv}} = \frac{R_y^{-1} a(\theta)}{a(\theta)^* R_y^{-1} a(\theta)}. \tag{1.5}$$

Equation (1.4) also differs from (1.2) in that the power expression we are minimizing includes the effect of the desired signal plus noise. The constraint $w^* a(\theta) = 1$ in (1.4) prevents the gain in the direction of the signal from being reduced.

A measure of the effectiveness of a beamformer is given by the signal-to-interference-plus-noise ratio, commonly abbreviated as SINR, given by

$$\mathrm{SINR} = \frac{\sigma_{\mathrm{d}}^2 |w^* a(\theta)|^2}{w^* R_v w}, \tag{1.6}$$

where σ_{d}^2 is the power of the signal of interest. The assumed value of the array manifold $a(\theta)$ may differ from the actual value for a host of reasons including imprecise knowledge of the signal's angle of arrival θ. Unfortunately, the SINR of Capon's method can degrade catastrophically for modest differences between the assumed and actual values of the array manifold. We now review several techniques for minimizing the sensitivity of MVB to modeling errors in the array manifold.

1.1.1 Previous Work

One popular method to address uncertainty in the array response or angle of arrival is to impose a set of unity-gain constraints for a small spread of angles around the nominal look direction. These are known in the literature as point mainbeam constraints or neighboring location constraints [2]. The beamforming problem with point mainbeam constraints can be expressed as

$$\begin{array}{ll} \text{minimize} & w^* R_y w \\ \text{subject to} & C^* w = f, \end{array} \tag{1.7}$$

where C is a $n \times L$ matrix of array responses in the L constrained directions and f is an $L \times 1$ vector specifying the desired response in each constrained direction. To achieve wider responses, additional constraint points are added. We may similarly constrain the derivative of the weighted array output to be zero at the desired look angle. This constraint can be expressed in the same framework as (1.7); in this case, we let C be the derivative of the array manifold with respect to look angle and $f = 0$. These are called *derivative mainbeam constraints*; this derivative may be approximated using regularization methods. Point and derivative mainbeam constraints may also be used in conjunction with one another. The minimizer of (1.7)

has an analytical solution given by

$$w_{\text{opt}} = R_y^{-1} C (C^* R_y^{-1} C)^{-1} f. \tag{1.8}$$

Each constraint removes one of the remaining degrees of freedom available to reject undesired signals; this is particularly significant for an array with a small number of elements. We may overcome this limitation by using a low-rank approximation to the constraints [3]. The best rank k approximation to C, in a least squares sense, is given by $U\Sigma V^*$, where Σ is a diagonal matrix consisting of the largest k singular values, U is a $n \times k$ matrix whose columns are the corresponding left singular vectors of C, and V is a $L \times k$ matrix whose columns are the corresponding right singular vectors of C. The reduced rank constraint equations can be written as $V\Sigma^T U^* w = f$, or equivalently

$$U^* w = \Sigma^\dagger V^* f, \tag{1.9}$$

where $\dagger$ denotes the Moore–Penrose pseudoinverse. Using (1.8), we compute the beamformer using the reduced rank constraints as

$$w_{\text{epc}} = R_y^{-1} U (U^* R_y^{-1} U)^{-1} \Sigma^\dagger V^* f.$$

This technique, used in source localization, is referred to as minimum variance beamforming with environmental perturbation constraints (MV-EPC), see Krolik [2] and the references contained therein.

Unfortunately, it is not clear how best to pick the additional constraints, or, in the case of the MV-EPC, the rank of the constraints. The effect of additional constraints on the design specifications appears difficult to predict.

Regularization methods [4] have also been used in beamforming. One technique, referred to in the literature as diagonal loading, chooses the beamformer to minimize the sum of the weighted array output power plus a penalty term, proportional to the square of the norm of the weight vector. The gain in the assumed angle of arrival (AOA) of the desired signal is constrained to be unity. The beamformer is chosen as the optimal solution of

$$\begin{array}{ll} \text{minimize} & w^* R_y w + \mu w^* w \\ \text{subject to} & w^* a(\theta) = 1. \end{array} \tag{1.10}$$

The parameter $\mu > 0$ penalizes large values of w and has the general effect of *detuning* the beamformer response. The regularized least squares problem (1.10) has an analytical solution given by

$$w_{\text{reg}} = \frac{(R_y + \mu I)^{-1} a(\theta)}{a(\theta)^* (R_y + \mu I)^{-1} a(\theta)}. \tag{1.11}$$

Gershman [5] and Johnson and Dudgeon [6] provide a survey of these methods; see also the references contained therein. Similar ideas have been used in adaptive algorithms, see Haykin [7].

Beamformers using eigenvalue thresholding methods to achieve robustness have also been used; see Harmanci et al. [8]. The beamformer is computed according to Capon's method, using a covariance matrix which has been modified to ensure no eigenvalue is less than a factor μ times the largest, where $0 \leq \mu \leq 1$. Specifically, let $V\Lambda V^*$ denote the eigenvalue/eigenvector decomposition of R_y, where Λ is a diagonal matrix, the ith entry (eigenvalue) of which is given by λ_i, that is,

$$\Lambda = \begin{bmatrix} \lambda_1 & & \\ & \ddots & \\ & & \lambda_n \end{bmatrix}.$$

Without loss of generality, assume $\lambda_1 \geq \lambda_2 \ldots \geq \lambda_n$. We form the diagonal matrix Λ_{thr}, the ith entry of which is given by $\max\{\mu\lambda_1, \lambda_i\}$; viz,

$$\Lambda_{\text{thr}} = \begin{bmatrix} \lambda_1 & & & \\ & \max\{\mu\lambda_1, \lambda_2\} & & \\ & & \ddots & \\ & & & \max\{\mu\lambda_1, \lambda_n\} \end{bmatrix}.$$

The modified covariance matrix is computed according to $R_{\text{thr}} = V\Lambda_{\text{thr}}V^*$. The beamformer using eigenvalue thresholding is given by

$$w_{\text{thr}} = \frac{R_{\text{thr}}^{-1}a(\theta)}{a(\theta)^*R_{\text{thr}}^{-1}a(\theta)}. \tag{1.12}$$

The parameter μ corresponds to the reciprocal of the condition number of the covariance matrix. A variation on this approach is to use a fixed value for the minimum eigenvalue threshold. One interpretation of this approach is to incorporate a priori knowledge of the presence of additive white noise when the sample covariance is unable to observe said white noise floor due to short observation time [8]. The performance of this beamformer appears similar to that of the regularized beamformer using diagonal loading; both usually work well for an appropriate choice of the regularization parameter μ.

We see two limitations with regularization techniques for beamformers. First, it is not clear how to efficiently pick μ. Second, this technique does not take into account any knowledge we may have about variation in the array manifold, for example, that the variation may not be isotropic.

In Section 1.1.3, we describe a beamforming method that explicitly uses information about the variation in the array response $a(\cdot)$, which we model explicitly as an uncertainty ellipsoid in $\mathbf{R}^{2n}$. Prior to this, we introduce some notation for describing ellipsoids.

1.1.2 Ellipsoid Descriptions

An n-dimensional ellipsoid can be defined as the image of an n-dimensional Euclidean ball under an affine mapping from $\mathbf{R}^n$ to $\mathbf{R}^n$; that is,

$$\mathcal{E} = \{Au + c \mid \|u\| \leq 1\}, \tag{1.13}$$

where $A \in \mathbf{R}^{n\times n}$ and $c \in \mathbf{R}^n$. The set $\mathcal{E}$ describes an ellipsoid whose center is c and whose *principal semiaxes* are the unit-norm left singular vectors of A scaled by the corresponding singular values. We say that an ellipsoid is *flat* if this mapping is not injective, that is, one-to-one. Flat ellipsoids can be described by (1.13) in the proper affine subspaces of $\mathbf{R}^n$. In this case, $A \in \mathbf{R}^{n\times l}$ and $u \in \mathbf{R}^l$. An interpretation of a flat uncertainty ellipsoid is that some linear combinations of the array manifold are known exactly [9].

Unless otherwise specified, an ellipsoid in $\mathbf{R}^n$ will be parameterized in terms of its center $c \in \mathbf{R}^n$ and a symmetric non-negative definite configuration matrix $Q \in \mathbf{R}^{n\times n}$ as

$$\mathcal{E}(c, Q) = \{Q^{1/2}u + c \mid \|u\| \leq 1\} \tag{1.14}$$

where $Q^{1/2}$ is any matrix square root satisfying $Q^{1/2}(Q^{1/2})^T = Q$. When Q is full rank, the nondegenerate ellipsoid $\mathcal{E}(c, Q)$ may also be expressed as

$$\mathcal{E}(c, Q) = \{x \mid (x - c)^T Q^{-1}(x - c) \leq 1\} \tag{1.15}$$

or by the equivalent quadratic function

$$\mathcal{E}(c, Q) = \{x \mid T(x) \leq 0\}, \tag{1.16}$$

where $T(x) = x^T Q^{-1}x - 2c^T Q^{-1}x + x_c^T Q^{-1}x_c - 1$. The first representation (1.14) is more natural when $\mathcal{E}$ is degenerate or poorly conditioned. Using the second description (1.15), one may easily determine whether a point lies within the ellipsoid. The third representation (1.16) will be used in Section 1.6.1 to compute the minimum-volume ellipsoid covering the union of ellipsoids.

We will express the values of the array manifold $a \in \mathbf{C}^n$ as the direct sum of its real and imaginary components in $\mathbf{R}^{2n}$; that is,

$$z_i = [\mathbf{Re}(a_1) \cdots \mathbf{Re}(a_n)\ \mathbf{Im}(a_1) \cdots \mathbf{Im}(a_n)]^T. \tag{1.17}$$

While it is possible to cover the field of values with a complex ellipsoid in $\mathbf{C}^n$, doing so implies a symmetry between the real and imaginary components which generally results in a larger ellipsoid than if the direct sum of the real and imaginary components are covered in $\mathbf{R}^{2n}$.

1.1.3 Robust Minimum Variance Beamforming

A generalization of (1.4) that captures our desire to minimize the weighted power output of the array in the presence of uncertainties in $a(\theta)$ is then:

$$\begin{array}{ll} \text{minimize} & w^* R_y w \\ \text{subject to} & \mathbf{Re}\ w^* a \geq 1\ \forall a \in \mathcal{E}, \end{array} \tag{1.18}$$

where **Re** denotes the real part. Here, $\mathcal{E}$ is an ellipsoid that covers the possible range of values of $a(\theta)$ due to imprecise knowledge of the array manifold $a(\cdot)$, uncertainty in the angle of arrival θ, or other factors. We shall refer to the optimal solution of (1.18) as the robust minimum variance beamformer (RMVB).

We use the constraint **Re** $w^* a \geq 1$ for all $a \in \mathcal{E}$ in (1.18) for two reasons. First, while normally considered a semi-infinite constraint, we show in Section 1.3 that it can be expressed as a second-order cone constraint. As a result, the robust minimum variance beamforming problem (1.18) can be solved reliably and efficiently. Second, the real part of the response is an efficient lower bound for the magnitude of the response, as the objective $w^* R_y w$ is unchanged if the weight vector w is multiplied by an arbitrary shift $e^{j\phi}$. This is particularly true when the uncertainty in the array response is relatively small. It is unnecessary to constrain the imaginary part of the response to be nominally zero.

Our approach differs from the previously mentioned beamforming techniques in that the weight selection uses the a priori uncertainties in the array manifold in a precise way; the RMVB is guaranteed to satisfy the minimum gain constraint for all values in the uncertainty ellipsoid.

Recently, several papers have addressed uncertainty in a similar framework. Wu and Zhang [10] observe that the array manifold may be described as a polyhedron and that the robust beamforming problem can be cast as a quadratic program. While the polyhedron approach is less conservative, the size of the description and hence the complexity of solving the problem grows with the number of vertices. Vorobyov et al. [11, 12] and Gershman [13] describe the use of second-order cone programming for robust beamforming in the case where the uncertainty is in the array response is isotropic, that is, a Euclidean ball. Our method, while derived differently, yields the same beamformer as proposed by Li et al. [14–16].

In this chapter, we consider the case in which the uncertainty is anisotropic [17–19]. We also show how the beamformer weights can be computed efficiently.

1.1.4 Outline of the Chapter

The rest of this chapter is organized as follows. In Section 1.2, we motivate the need for robustness with a simple array which includes the effect of coupling between antenna elements. In Section 1.3 we discuss the RMVB. A numerically efficient technique based on Lagrange multiplier methods is described; we will see that the RMVB can be computed with the same order of complexity as its nonrobust counterpart. A numerical example is given in Section 1.4. In Section 1.5 we describe

ellipsoidal modeling methods which make use of simulated or measured values of the array manifold. In Section 1.6 we discuss more sophisticated techniques, based on ellipsoidal calculus, for propagating uncertainty ellipsoids. In particular, we describe a numerically efficient method for approximating the numerical range of the Hadamard (element-wise) product of two ellipsoids. This form of uncertainty arises when the array outputs are subject to multiplicative uncertainties. A numerical beamforming example considering multiplicative uncertainties is given in Section 1.7. Our conclusions are given in Section 1.8.

1.2 A PRACTICAL EXAMPLE

Our goals for this section are twofold:

- To make the case that antenna elements may behave *very* differently in free space than as part of closely spaced arrays, and
- To motivate the need for robustness in beamforming.

Consider the four-element linear array of half-wave dipole antennas depicted in Figure 1.2. Let the frequency of operation be 900 MHz and the diameter of the

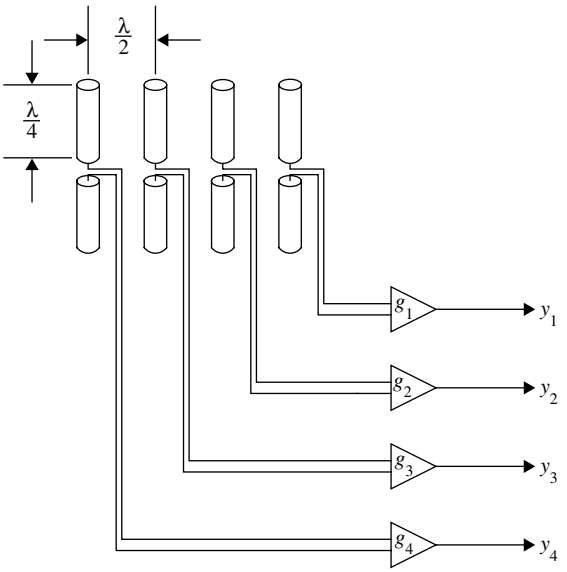

Figure 1.2 The four-element array. For this array, we simulate the array response which includes the effect of coupling between elements. In this example, the gains $g_1, \ldots, g_4$ are all assumed nominal. Later we consider the effect of multiplicative uncertainties.

elements be 1.67 mm. Assume each dipole is terminated into a 100 ohm load. The length of the dipole elements was chosen such that an isolated dipole in free space matched this termination impedance.

The array was simulated using the Numerical Electromagnetics Code, version 4 (NEC-4) [20]. Each of the radiating elements was modeled with six wire segments. The nominal magnitude and phase responses are given in Figures 1.3 and 1.4, respectively. Note that the amplitude is *not* constant for all angles of arrival or the same for all elements. This will generally be the case with closely spaced antenna elements due to the high level of interelement coupling.

In Figure 1.5, we see that the vector norm of the array response is *not* a constant function of AOA, despite the fact that the individual elements, in isolation, have an isotropic response.

Next, let us compare the performance of the RMVB with Capon's method using this array, with nominal termination impedances. Assume the desired signal impinges on the array from an angle $\theta_{\text{sig}} = 127^\circ$ and has a signal-to-noise ratio (SNR) of 20 decibels (dB). We assume that an interfering signal arrives at an

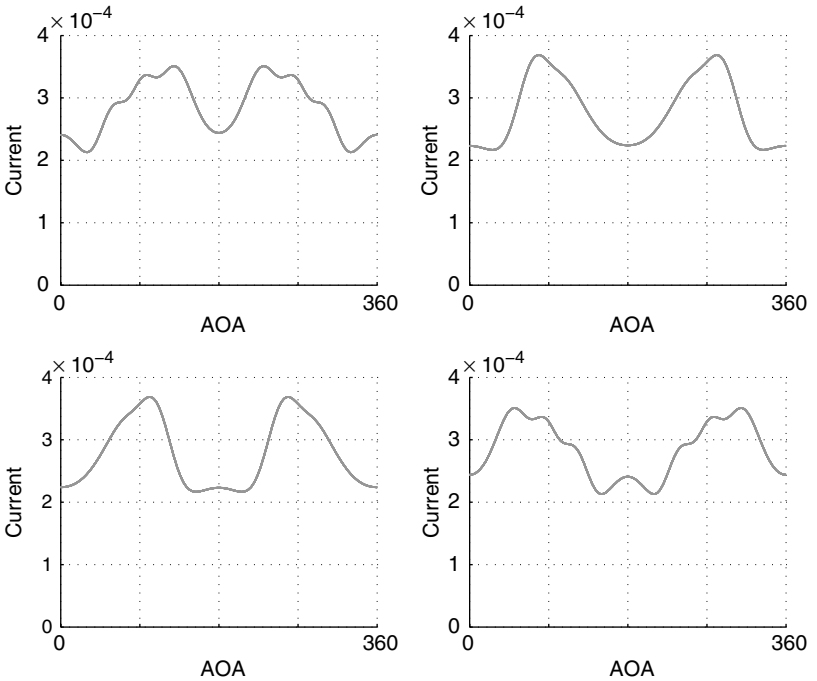

Figure 1.3 Magnitude of response of four-element array consisting of half-wave dipoles with uniform spacing of $\lambda/2$. The currents have units of amperes for a field strength of 1 volt/meter. The angle of arrival (AOA) is in degrees. Note the symmetry of the response. The outer elements correspond to the top left and bottom right plots; the inner elements, top right and lower left.

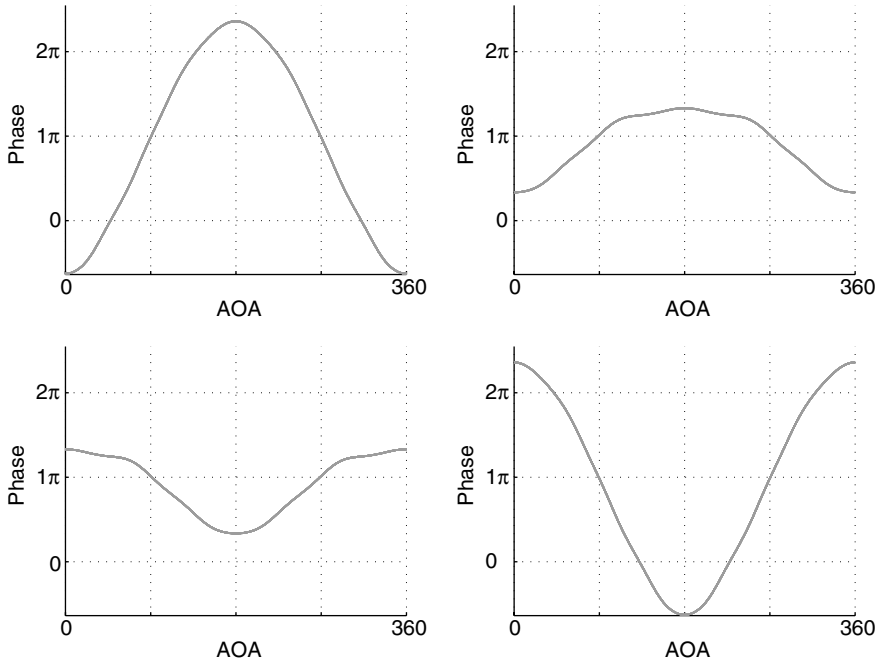

Figure 1.4 Phase response, in radians, of the four-element half-wave dipole array. The angle of arrival is in degrees. Again, note the symmetry in the response.

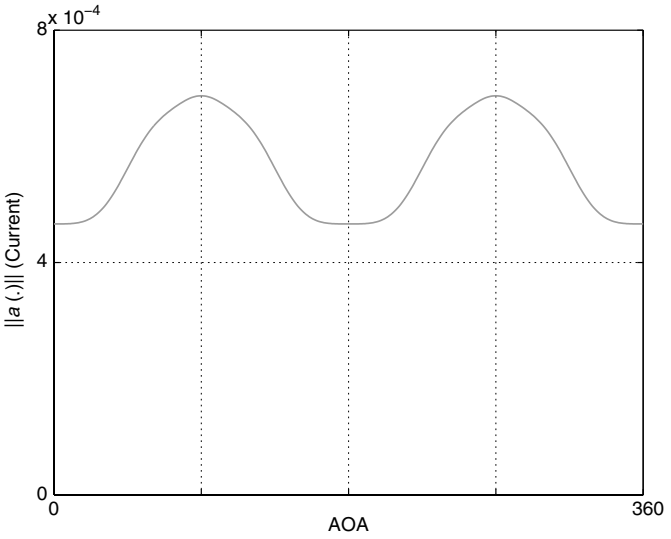

Figure 1.5 The vector norm of the array response as a function of AOA. Note that the norm is not constant despite the fact that each of the elements are isotropic with respect to AOA.

angle of $\theta_{\text{int}} = 150^\circ$ with amplitude twice that of the desired signal. For Capon's method, we assume an AOA of $\theta_{\text{nom}} = 120^\circ$. For the RMVB, we compute a minimum-volume ellipsoid covering the numerical range of the array manifold for all angles of arrival between 112° and 128°. The details of this calculation will be described in Section 1.5. Let $w_{\text{mv}} \in \mathbf{C}^4$ denote the beamformer vector produced by Capon's method and $w_{\text{rmvb}} \in \mathbf{C}^4$ the robust minimum-variance beamformer, that is, the optimal solution of (1.18).

A plot of the response of the minimum-variance beamformer (MVB) and the robust minimum-variance beamformer (RMVB) as a function of angle of arrival is shown in Figure 1.6. By design, the response of the MVB has unity gain in the direction of the assumed AOA, that is, $w_{\text{mv}}^* a(\theta_{\text{nom}}) = 1$, where $a : \mathbf{R} \to \mathbf{C}^4$ denotes the array manifold. The MVB produces a deep null in the direction of the interference: $w_{\text{mv}}^* a(\theta_{\text{int}}) = -0.0061 + 0i$. Unfortunately, the MVB also strongly attenuates the desired signal, with $w_{\text{mv}}^* a(\theta_{\text{sig}}) = -0.0677 + 0i$. The resulting post-beamforming signal-to-interference-plus-noise ratio (SINR) is -10.5 dB, appreciably worse than the SINR obtained using a single antenna *without* beamforming.

While the robust beamformer does not cast as deep a null in the direction of the interfering signal, that is, $w_{\text{rmvb}}^* a(\theta_{\text{int}}) = -0.0210 + 0i$, it maintains greater than unity gain for all angles of arrival in our design specification. The SINR obtained using the RMVB is 12.4 dB.

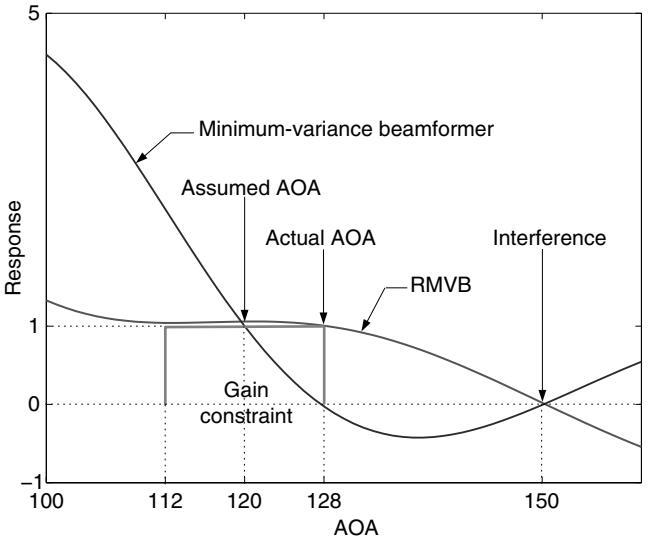

Figure 1.6 The response of the minimum-variance beamformer (Capon's method) and the robust minimum-variance beamformer (RMVB). The a priori uncertainty in the angle of arrival (AOA) was $\pm 8^\circ$. We see that the RMVB maintains at least unity gain for all angles in this range, whereas Capon's method fails for an AOA of approximately 127°.

When the actual AOA of the desired signal equals the assumed 120°, the SINR of the MVB is an impressive 26.5 dB, compared to 10.64 dB for the RMVB. It is tempting then to consider methods to reduce the uncertainty and potentially realize this substantial improvement in SINR. Such efforts are unlikely to be fruitful. For example, a 1° error in the assumed AOA reduces the SINR of Capon's method by more than 20 dB to 4.0 dB. Also, the mathematical values of the array model differ from the actual array response for a number of reasons, of which error in the assumed AOA is but one. In the presence of array calibration errors, variations due to termination impedances, and multiplicative gain uncertainties, nonrobust techniques simply do not work reliably.

In our example, we considered only uncertainty in the angle of arrival; verifying the performance for the nonrobust method involved evaluating points in a one-dimensional interval. Had we considered the additional effect of multiplicative gain variations, for example, the numerical cost of verifying the performance of the beamformer for a dense grid of possible array values could dwarf the computational complexity of the robust method. The approach of the RMVB is different; it makes specific use of the uncertainty in the array response. We compute either a worst-case optimal vector for the ellipsoidal uncertainty region or a proof that the design specification is infeasible. No subsequent verification of the performance is required.

1.3 ROBUST WEIGHT SELECTION

Recall from Section 1.1 that the RMVB was the optimal solution to

$$\begin{array}{ll} \text{minimize} & w^* R_y w \\ \text{subject to} & \mathbf{Re}\ w^* a \geq 1\ \forall a \in \mathcal{E}. \end{array} \tag{1.19}$$

For purposes of computation, we will express the weight vector w and the values of the array manifold a as the direct sum of the corresponding real and imaginary components

$$x = \begin{bmatrix} \mathbf{Re}\ w \\ \mathbf{Im}\ w \end{bmatrix} \quad \text{and} \quad z = \begin{bmatrix} \mathbf{Re}\ a \\ \mathbf{Im}\ a \end{bmatrix}. \tag{1.20}$$

The real and imaginary components of the product $w^* a$ can be expressed as

$$\mathbf{Re}\ w^* a = x^T z \tag{1.21}$$

and

$$\mathbf{Im}\ w^* a = x^T U z, \tag{1.22}$$

where U is the orthogonal matrix

$$U = \begin{bmatrix} 0 & I_n \\ -I_n & 0 \end{bmatrix},$$

and I_n is an $n \times n$ identity matrix. The quadratic form $w^* R_y w$ may be expressed in terms of x as $x^T R x$, where

$$R = \begin{bmatrix} \mathbf{Re}\, R_y & -\mathbf{Im}\, R_y \\ \mathbf{Im}\, R_y & \mathbf{Re}\, R_y \end{bmatrix}.$$

Assume R is positive definite; with sufficient sample support, it is with probability - one.

Let $\mathcal{E} = \{Au + c \mid \|u\| \leq 1\}$ be an ellipsoid covering the possible values of x, that is, the real and imaginary components of a. The ellipsoid $\mathcal{E}$ is centered at c; the matrix A determines its size and shape. The constraint $\mathbf{Re}\ w^* a \geq 1$ for all $a \in \mathcal{E}$ in (1.18) can be expressed

$$x^T z \geq 1 \quad \forall z \in \mathcal{E}, \tag{1.23}$$

which is equivalent to

$$u^T A^T x \leq c^T x - 1 \text{ for all } u \text{ s.t.}, \quad \|u\| \leq 1. \tag{1.24}$$

Now, (1.24) holds for all $\|u\| \leq 1$ if and only if it holds for the value of u that maximizes $u^T A^T x$, namely $u = A^T x / \|A^T x\|$. By the Cauchy-Schwartz inequality, we see that (1.23) is equivalent to the constraint

$$\|A^T x\| \leq c^T x - 1, \tag{1.25}$$

which is called a *second-order cone constraint* [21]. We can then express the robust minimum-variance beamforming problem (1.18) as

$$\begin{aligned} &\text{minimize} \quad x^T R x \\ &\text{subject to} \quad \|A^T x\| \leq c^T x - 1, \end{aligned} \tag{1.26}$$

which is a second-order cone program. See references [21–23]. The subject of robust convex optimization is covered in references [9, 24–28].

By assumption, R is positive definite and the constraint $\|A^T x\| \leq c^T x - 1$ in (1.26) precludes the trivial minimizer of $x^T R x$. Hence, this constraint will be tight for any optimal solution and we may express (1.26) in terms of real-valued

quantities as

$$\begin{aligned} &\text{minimize} \quad x^T R x \\ &\text{subject to} \quad c^T x = 1 + \|A^T x\|. \end{aligned} \tag{1.27}$$

Compared to the MVB, the RMVB adds a margin that scales with the size of the uncertainty. In the case of no uncertainty where $\mathcal{E}$ is a singleton whose center is $c = [\mathbf{Re}\, a(\theta_d)^T \;\; \mathbf{Im}\, a(\theta_d)^T]^T$, (1.27) reduces to Capon's method and admits an analytical solution given by the MVB (1.5). Unlike the use of additional point or derivative mainbeam constraints or a regularization term, the RMVB is guaranteed to satisfy the minimum gain constraint for all values in the uncertainty ellipsoid. In the case of isotropic array uncertainty, the optimal solution of (1.18) yields the same weight vector (to a scale factor) as the regularized beamformer for the proper the proper choice of μ.

1.3.1 Lagrange Multiplier Methods

We may compute the RMVB efficiently using Lagrange multiplier methods. See, for example, references [29–30], [31, §12.1.1], and [32]. The RMVB is the optimal solution of

$$\begin{aligned} &\text{minimize} \quad x^T R x \\ &\text{subject to} \quad \|A^T x\|^2 = (c^T x - 1)^2 \end{aligned} \tag{1.28}$$

if we impose the additional constraint that $c^T x \geq 1$. We define the *Lagrangian* L: $\mathbf{R}^n \times \mathbf{R} \to \mathbf{R}$ associated with (1.28) as

$$\begin{aligned} L(x, \lambda) &= x^T R x + \lambda\left(\|A^T x\|^2 - (c^T x - 1)^2\right) \\ &= x^T (R + \lambda Q) x + 2\lambda c^T x - \lambda, \end{aligned} \tag{1.29}$$

where $Q = AA^T - cc^T$. To calculate the stationary points, we differentiate $L\,(x, y)$ with respect to x and λ; setting these partial derivatives equal to zero yields the Lagrange equations:

$$(R + \lambda Q)x = -\lambda c \tag{1.30}$$

and

$$x^T Q x + 2c^T x - 1 = 0. \tag{1.31}$$

To solve for the Lagrange multiplier λ, we note that equation (1.30) has an analytical solution given by

$$x = -\lambda (R + \lambda Q)^{-1} c;$$

applying this to (1.31) yields

$$f(\lambda) = \lambda^2 c^T (R + \lambda Q)^{-1} Q (R + \lambda Q)^{-1} c - 2\lambda c^T (R + \lambda Q)^{-1} c - 1. \tag{1.32}$$

The optimal value of the Lagrange multiplier λ^* is then a zero of (1.32). We proceed by computing the eigenvalue/eigenvector decomposition

$$V \Gamma V^T = R^{-1/2} Q (R^{-1/2})^T$$

to diagonalize (1.32), that is,

$$f(\lambda) = \lambda^2 \bar{c}^T (I + \lambda \Gamma)^{-1} \Gamma (I + \lambda \Gamma)^{-1} \bar{c} - 2\lambda \bar{c}^T (I + \lambda \Gamma)^{-1} \bar{c} - 1, \tag{1.33}$$

where $\bar{c} = V^T R^{-1/2} c$. Equation (1.33) reduces to the following scalar *secular* equation:

$$f(\lambda) = \lambda^2 \sum_{i=1}^{n} \frac{\bar{c}_i^2 \gamma_i}{(1 + \lambda \gamma_i)^2} - 2\lambda \sum_{i=1}^{n} \frac{\bar{c}_i^2}{(1 + \lambda \gamma_i)} - 1, \tag{1.34}$$

where $\gamma \in \mathbf{R}^n$ are the diagonal elements of Γ. The values of γ are known as the *generalized eigenvalues* of Q and R and are the roots of the equation $\det(Q - \lambda R) = 0$. Having computed the value of λ^* satisfying $f(\lambda^*) = 0$, the RMVB is computed according to

$$x^* = -\lambda^* (R + \lambda^* Q)^{-1} c. \tag{1.35}$$

Similar techniques have been used in the design of filters for radar applications; see Stutt and Spafford [33] and Abramovich and Sverdlik [34].

In principle, we could solve for all the roots of (1.34) and choose the one that results in the smallest objective value $x^T R x$ *and* satisfies the constraint $c^T x > 1$, assumed in (1.28). In the next section, however, we show that this constraint is only met for values of the Lagrange multiplier λ greater than a minimum value, $\lambda_{\min}$. We will see that there is a single value of $\lambda > \lambda_{\min}$ that satisfies the Lagrange equations.

1.3.2 A Lower Bound on the Lagrange Multiplier

We begin by establishing the conditions under which (9) has a solution. Assume $R = R^T \succ 0$, that is, R is symmetric and positive definite.

Lemma 1. For $A \in \mathbf{R}^{n \times n}$ full rank, there exists an $x \in \mathbf{R}^n$ for which $\|A^T x\| = c^T x - 1$ if and only if $c^T (A A^T)^{-1} c > 1$.

Proof. To prove the if direction, define

$$x(\lambda) = (c c^T - A A^T - \lambda^{-1} R)^{-1} c. \tag{1.36}$$

By the matrix inversion lemma, we have

$$\begin{aligned} c^T x(\lambda) - 1 &= c^T (cc^T - AA^T - \lambda^{-1} R)^{-1} c - 1 \\ &= \frac{1}{c^T (AA^T + \lambda^{-1} R)^{-1} c - 1}. \end{aligned} \tag{1.37}$$

For $\lambda > 0$, $c^T (AA^T + \lambda^{-1} R)^{-1} c$ is a monotonically increasing function of λ; therefore, for $c^T (AA^T)^{-1} c > 1$, there exists a $\lambda_{\min} \in \mathbf{R}^+$ for which

$$c^T (AA^T + \lambda_{\min}^{-1} R)^{-1} c = 1. \tag{1.38}$$

This implies that the matrix $(R + \lambda_{\min} Q)$ is singular. Since

$$\begin{aligned} \lim_{\lambda \to \infty} c^T x(\lambda) - 1 &= -c^T (AA^T - cc^T)^{-1} c - 1 \\ &= \frac{1}{c^T (AA^T)^{-1} c - 1} > 0, \end{aligned}$$

$c^T x(\lambda) - 1 > 0$ for all $\lambda > \lambda_{\min}$.

As in (1.32) and (1.34), let $f(\lambda) = \|A^T x\|^2 - (c^T x - 1)^2$. Examining (1.32), we see

$$\begin{aligned} \lim_{\lambda \to \infty} f(\lambda) &= -c^T (AA^T - cc^T)^{-1} c - 1 \\ &= \frac{1}{c^T (AA^T)^{-1} c - 1} > 0. \end{aligned}$$

Evaluating (1.32) or (1.34), we see $\lim_{\lambda \to \lambda_{\min}^+} f(\lambda) = -\infty$. For all $\lambda > \lambda_{\min}$, $c^T x > 1$ and $f(\lambda)$ is continuous. Hence $f(\lambda)$ assumes the value of 0, establishing the existence of a $\lambda > \lambda_{\min}$ for which $c^T x(\lambda) - 1 = \|A^T x(\lambda)\|$.

To show the only if direction, assume x satisfies $\|A^T x\| \leq c^T x - 1$. This condition is equivalent to

$$z^T x \geq 1 \forall z \in \mathcal{E} = \{Au + c \mid \|u\| \leq 1\}. \tag{1.39}$$

For (1.39) to hold, the origin cannot be contained in ellipsoid $\mathcal{E}$, which implies $c^T (AA^T)^{-1} c > 1$. □

REMARK. The constraints $(c^T x - 1)^2 = \|A^T x\|^2$ and $c^T x - 1 > 0$ in (1.28), taken together, are equivalent to the constraint $c^T x - 1 = \|A^T x\|$ in (1.27). For $R = R^T \succ 0$, A full rank and $c^T (AA^T)^{-1} c > 1$, (1.27) has a unique minimizer x^*. For $\lambda > \lambda_{\min}$, $(\lambda^{-1} R + Q)$ is full rank, and the Lagrange equation (1.30)

$$(\lambda^{-1} R + Q) x^* = -c$$